Sensors & Transducers, Vol. 203, Issue 8, August 2016, pp. 33-39

Sensors & Transducers

http://www.sensorsportal.com

Point-of-care Devices: Non-Newtonian Whole Blood Behavior and Capillary Flow on Reagent-coated Walls

[1, *] Jean BERTHIER, [1] David GOSSELIN, [1] Maxime HUET, [2] Gwenola SABATTE, [2] Patrick POUTEAU, [1] Fabrice NAVARRO and [1] Myriam CUBIZOLLES

[1] Univ. Grenoble Alpes F-38000 Grenoble, France
[1] CEA, LETI, MINATEC Campus, F-38054, Grenoble, France
[2] Avalun, Grenoble, France
[*] E-mail: jean.berthier@cea.fr

Received: 29 July 2016 /Accepted: 28 August 2016 /Published: 31 August 2016

Abstract: Most point-of-care (POC) and patient self-testing (PST) devices are based on the analysis of whole blood taken from a finger prick. Whole blood contains a bountiful of information about the donor's health. We analyze here two particularities of microsystems for blood analysis: the blood non-Newtonian behavior, and the capillary flow in reagent-coated channels.

Capillarity is the most commonly used method to move fluids in portable systems. It is shown first that the capillary flow of blood does not follow the Lucas-Washburn-Rideal law when the capillary flow velocity is small, due to its non-Newtonian rheology and to the formation of rouleaux of RBCs.

In a second step, the capillary flow of blood on reagent-coated surfaces is investigated; first experimentally by observing the spreading of a droplet of blood on different reagent-coated substrates; second theoretically and numerically using the general law for spontaneous capillary flows and the Evolver numerical program.

Keywords: Whole blood, Point-of-care systems, Non-Newtonian flow, Reagent, RBC rouleaux, Hoffman-Voinov-Tanner (HVT) law, Lucas-Washburn-Rideal (LWR) law, Spontaneous capillary flow (SCF).

1. Introduction

Point-of-care (POC) and patient self-testing (PST) devices are interesting tools for the monitoring of people health, early detection of diseases, and adjustment of a treatment [1-3]. Most point-of-care (POC) and patient self-testing (PST) devices are based on the analysis of whole blood taken from a finger prick. Whole blood contains a bountiful of information about the donor's health: some are contained in the blood plasma, others are carried by the red blood cells (RBC). Metabolites, such as glucose and cholesterol, are transported by the plasma; pathogens, parasites, viruses and bacteria are also found in the plasma [4-5]. On the other hand, RBCs count, circulating tumoral cells characterize the cellular phase [6].

Most of the time, portable systems use capillary forces to move the samples [1-3, 7]. We analyze here two fundamental characteristics of such systems for blood analysis: the blood non-Newtonian behavior [8], and the capillary flow in reagent-coated channels.

It is shown here that the capillary flow of blood does not follow the Lucas-Washburn-Rideal law

(LWR) and its non-cylindrical extension [9-10] when the capillary flow velocity is small, due to its non-Newtonian rheology and to the formation of rouleaux of RBCs [11].

In a second step, the capillary flow of blood on reagent-coated surfaces is investigated; first experimentally by observing the spreading of a droplet of blood on different reagent-coated substrates (IgM, dye, enzymes, surfactants, SLS [12]), second theoretically and numerically using the general law for spontaneous capillary flows and the Evolver numerical program [13].

2. Whole Blood Non-Newtonian Behavior

The dynamics of whole blood flow is related to its viscosity. Whole blood rheology is complicated. It depends on many parameters, such as hematocrit and fibrinogen levels. A law for viscosity as a function of the shear rate is the Casson law [8], or the more general Herschel-Bulkley law [14] (Fig. 1).

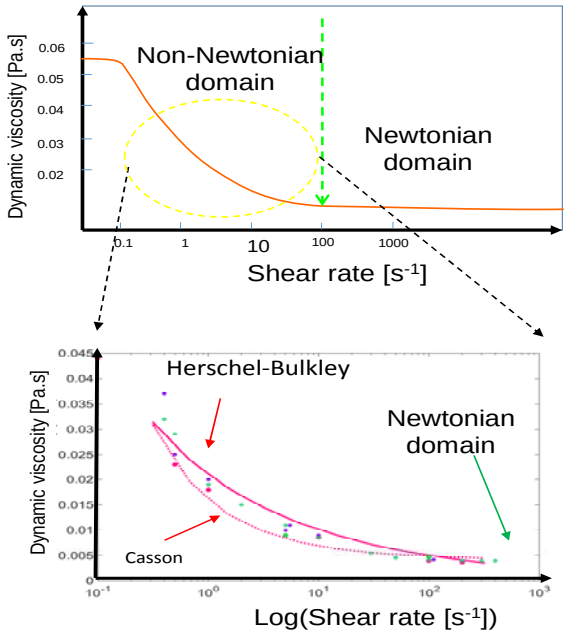

Fig. 1. Dynamic viscosity of whole blood as a function of the shear rate (top), showing a shear-thinning behavior; blow-up on the shear-thinning of whole blood (bottom): the dots correspond to experimental data found in the literature, the two curves are the Herschel-Bulkley and Casson formulas.

When the shear rate is small, rouleaux of RBCs form, giving the blood a strong non-Newtonian, yield stress behavior (Fig. 2(a) and Fig. 2(b)) [11, 15].

Whole blood capillary flow has been studied using a simple capillary tube of 100 μm diameter plugged to an open inlet port (Fig. 3). The velocity and penetration of the flow are monitored by following the position of the advancing interface using a millimetric paper.

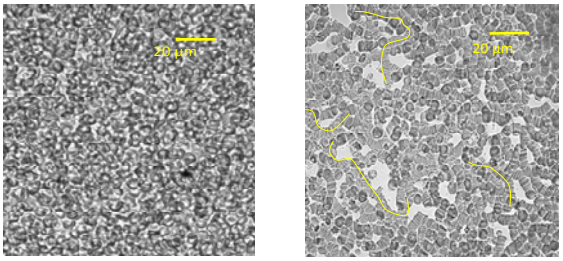

(a) (b)

Fig. 2. (a) Dispersed whole blood; (b) Whole blood forming "rouleaux" (the yellow lines show some of the rouleaux).

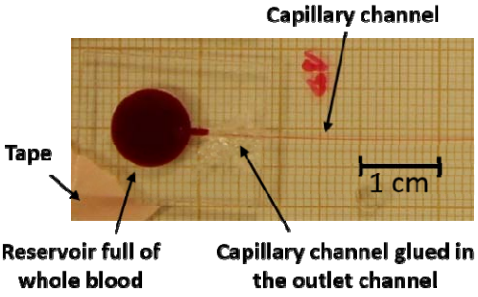

Fig. 3. View of the cylindrical tube plugged to the reservoir.

At the beginning of the capillary flow, velocities are sufficiently high to produce shear rates larger than the threshold of approximately $\dot{\gamma}_{th} \sim 100$ s^{-1} characterizing the Newtonian-viscoelastic transition (Fig. 1). The penetration distance obeys the LWR law for a tube of radius R:

$$z = \sqrt{\frac{\gamma}{\mu}\frac{R}{2}\cos\theta}\ \sqrt{t}\,, \tag{1}$$

where γ is the surface tension, μ is the viscosity (Newtonian) and θ is the contact angle. The flow being a laminar Poiseuillle flow upstream from the meniscus, the wall shear rate is

$$\dot{\gamma} = \frac{4V}{R} \tag{2}$$

Upon substitution of (1), relation (2) becomes

$$\dot{\gamma} = \frac{4}{R}\frac{dz}{dt} = \frac{4}{R}\left(\frac{\gamma}{\mu}\frac{R}{4}\cos\theta\,\frac{1}{z}\right) \tag{3}$$

After a distance z_t characterized by

$$z_t \approx \frac{\gamma}{\mu\,\dot{\gamma}_{th}}\cos\theta\,, \tag{4}$$

the flow becomes non-Newtonian and LWR law is no more verified (Fig. 4): The capillary flow of whole

blood departs from the Lucas-Washburn-Rideal law for large penetration distances. This viscoelastic behavior is associated to the formation of rouleaux [11, 16].

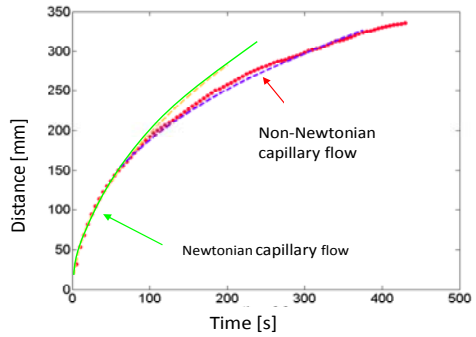

(a)

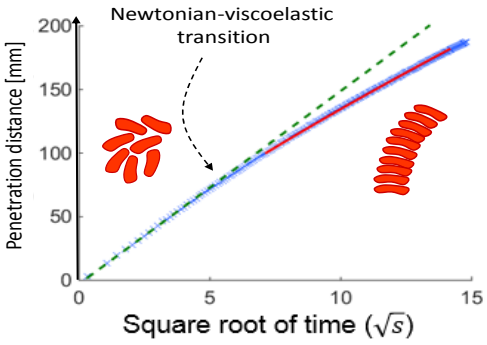

(b)

Fig. 4. Penetration distance vs. elapsed time: (a) Penetration distance as a function of time showing Newtonian and non-Newtonian behavior: red dots correspond to the experimental results, the green line corresponds to the LWR law, violet discontinuous line to the viscoelastic regime using the equation proposed in [16]; (b) Penetration distance as a function of square root of time: The blue dots correspond to the experimental observations, the green dotted line to the LWR law, the red line results from a model for the viscoelastic regime. In the Newtonian regime RBCs are dispersed, while they form rouleaux in the viscoelastic regime.

The travel distance of a capillary flow of Herschel-Bulkley liquid (such as whole blood) in a tube has been derived by Gosselin and coworkers in [16], and is the solution of a differential equation that reduces to the Weissenberg-Rabinowitsch-Mooney equation for power-law fluids, and to the Lucas-Washburn-Rideal law for Newtonian fluids.

3. Capillary Flow on Reagent-coated Walls

Point-of-care or home-care systems need embedded reagents, coated on the walls or lyophilized [17-18]. Dry coatings modify both the geometry of the channel and their surface energy, resulting in a change of the capillary flow [19]. We first analyze the spreading of whole blood on different reagent-coated surfaces, and then the capillary flow of whole blood in reagent-coated channels.

3.1. Spreading of Whole Blood on Different Reagent-coated Surfaces

Experiments have been conducted to observe the spreading of whole blood on different substrates: uncoated COP (cyclo-olefin polymer), COP coated with IgM and dyes containing various excipients.

The principle is illustrated in Fig. 5 where droplets of reagent (6-10 µl) are first deposited on the COP substrate, then spread and finally dry. Next a few µl blood droplet (2-6 µl) is deposited in the middle of the dried reagent stain (Fig. 5(b)).

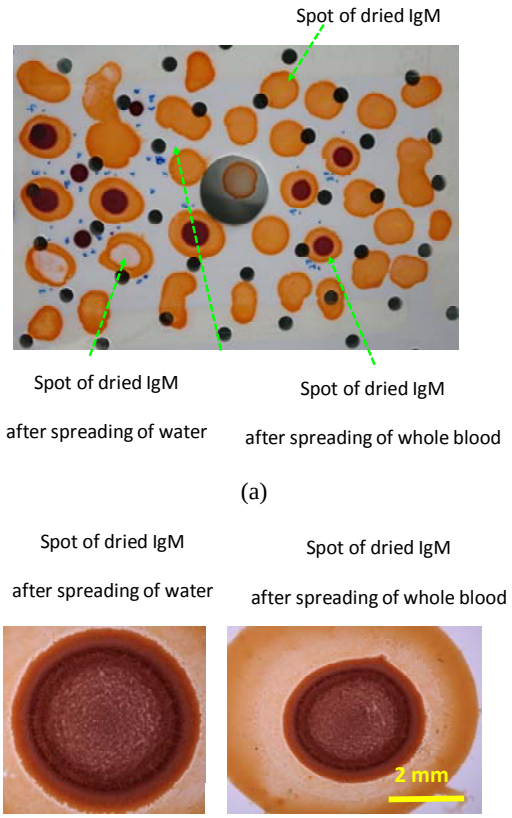

(a)

(b)

Fig. 5. (a) A COP plate coated with droplets of dried reagents, such as IgM; (b) Spreading (and drying) of a droplet of blood deposited on IgM coated substrate.

The spreading was observed using a Drop Shape Analyzer (DSA100, Krüss, Germany). As shown in Fig. 6, the droplet first touches the flat substrate, then spreads. Often whole blood forms a thread before total release due to the strong viscoelastic behavior [20].

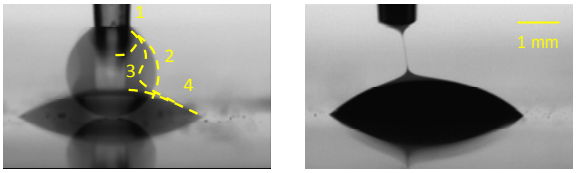

(a) (b)

Fig. 6. Spreading of whole blood on reagent coated surfaces: (a) Initial contours of the droplet detaching from the pipette (1, 2, 3, 4 are the successive contours of the drop); (b) Spreading showing the formation of a thread.

It was checked that the Hoffman-Voinov-Tanner law is approximately verified for whole blood spreading on reagent coated surfaces [21-22]. The kinetics of the advancing contact angle $\theta_a(t)$ is monitored and a static contact angle θ_s is determined at the end of the spreading motion. Fig. 7 shows the different kinetics of spreading depending on the coatings.

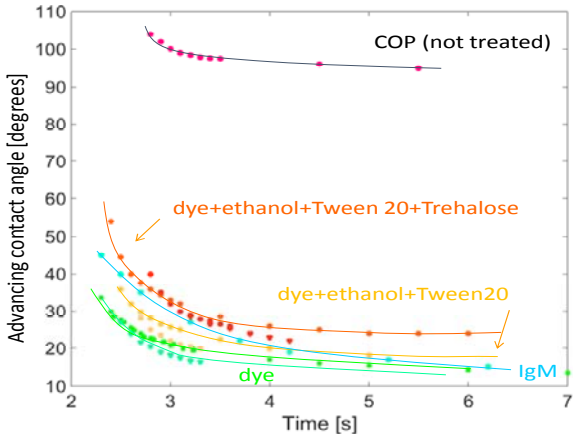

Fig. 7. Kinetics of spreading of whole blood on different reagent coated surfaces. Tween 20 is a surfactant, trehalose a dissacharide, IgM is n immoglobuline M and the "dye" is a chromogenic indicator for oxydoreductase. The dots correspond to the measured contact angles and the continuous lines are guides for the eyes.

The location of the advancing triple line $z(t)$ is recorded, which produces the spreading velocity $V(t)$. Eliminating the time, a plot of the dynamic contact angle as a function of the capillary number can be drawn. It is checked that the Hoffmann-Voinov-Tanner law is satisfactorily respected (Fig. 8), i.e.

$$\theta_a^3 - \theta_s^3 \cong c\,Ca \qquad (5)$$

Hence an advancing contact angle is determined as a function of the velocity: $\theta_a \cong \sqrt[3]{c\,Ca + \theta_s^3}$.

It has been shown that the advancing contact angle in a capillary flow decreases to the static value within a penetration distance smaller than few hydraulic diameters [23-24]. Hence, the value of the static Young contact angle θ_s is of great interest and is given by the horizontal limit in Fig. 7.

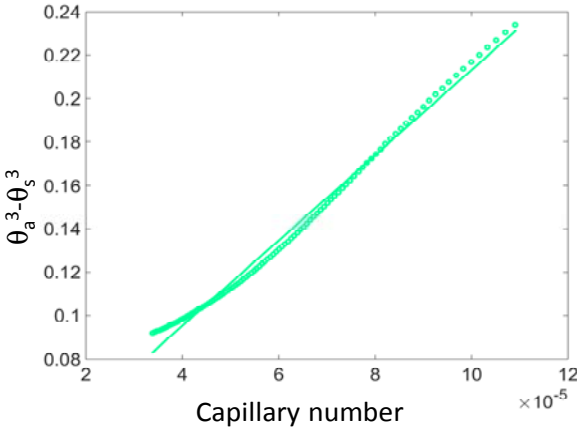

Fig. 8. HVT law is respected during the spreading of whole blood on an IgM coated surface.

3.2. Capillary Flow on Reagent-coated Surfaces

Point-of-care (POC) or patient self testing (PST) devices require the use of reagents to achieve the biological assays. These reagents can be lyophilized or dried. We focus here on dried reagents and we assume that their dissolution is not instantaneous upon arrival of the blood [25-26].

Reagent functionalization of the device is first achieved by introducing liquid reagent in the device. There are different approaches to introduce liquid reagent. Either the reagent can be deposited locally with a pipette or a robot (Fig. 9) [27], and the device is closed afterwards, or reagent must fill the reaction chamber using capillary motion, in the case of an already closed system.

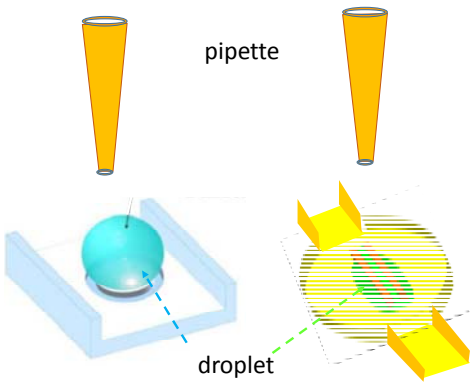

Fig. 9. Different methods of deposition of liquid reagents locally in a capillary microfluidics device. Left: Fuchiwaki, *et al.* approach where the droplet is pipetted on a circular surface surrounded by a micro-ditch [27], right: another solution for immobilizing reagents, in which the droplet is pipetted between two ridges.

Note that the coating is usually not uniform: In the case of interior concave corners, the drying process concentrates the reagents in these corners [7, 26] (Fig. 10).

The presence of dried-coating layers modifies the subsequent capillary filling with whole blood. There are two effects: a chemical effect associated to the change of surface energy introduced by the coating, and a geometrical effect associated to the deposit of solid coating. This geometrical change of sharpness of the interior corners impedes the development of capillary filaments [28-30], and the capillary filling may become impossible if the component is not well designed.

The occurrence of spontaneous capillary flow (SCF) has been theoretically determined and numerical and experimental validations have been performed [12, 18, 29, 31]. We make here the assumption that the spreading is fast compared to the re-dissolution of the coating.

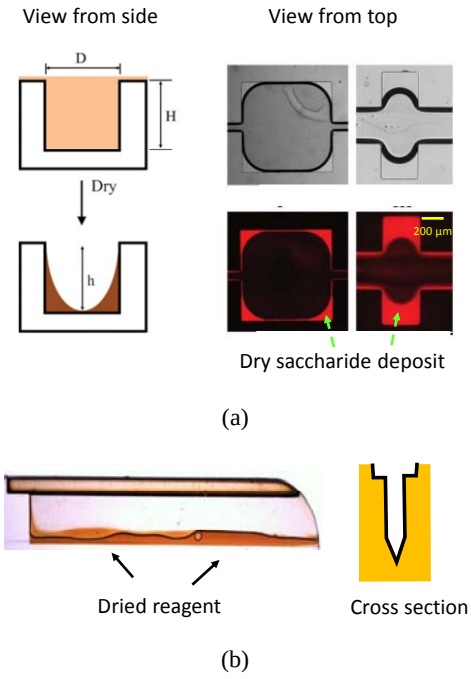

Fig. 10. (a) Dried coating of a channel with monosaccharide such as D-glucose or D-sorbitol showing concentration of solid monosaccharide in the corners [26]; (b) Dried coating of IgM in a V-groove showing concentration of IgM in the tip of the V-groove [7].

The general SCF condition in absence of capillary filaments in composite channels is given by the extended Cassie relation proposed by Berthier and Brakke [19]

$$f_{not-coated}\ \cos\theta_{B,W} + f_{coated}\ \cos\theta_{B,R} > f_{air}\,, \qquad (6)$$

where the coefficients f are the fractions of the cross section lengths of different wettabilities, and the contact angles $\theta_{B,W}$ et $\theta_{B,R}$ are the wall and reagent-coated wall contact angles with blood respectively. We assume here that the capillary number is small and consequently that the advancing contact angles are equal to the static ones, which is usually valid for capillary flow [23-24].

Before the blood is introduced, the reagent must fill the device. Hence the second condition for the SCF of reagent

$$\left(f_{not-coated} + f_{coated}\right)\cos\theta_{R,W} > f_{air}\,, \qquad (7)$$

where $\theta_{R,W}$ is the contact angle between reagent and wall. The design must then satisfy the matrix inequality

$$\begin{bmatrix}\cos\theta_{B,W} & \cos\theta_{B,R}\\ \cos\theta_{R,W} & \cos\theta_{R,W}\end{bmatrix}\begin{Bmatrix}f_{not-coated}\\ f_{coated}\end{Bmatrix} > \begin{Bmatrix}f_{air}\\ f_{air}\end{Bmatrix} \qquad (8)$$

Let us consider a V-groove, with the three different morphologies of reagent deposit in the dihedral shown in Fig. 11: (A) shows the uncoated groove, (B) corresponds to a uniform coating of the groove dihedral, (C) to a flat filling of the dihedral bottom – which we will call trapezoidal filling, (D) to a rounded filling of the dihedral bottom.

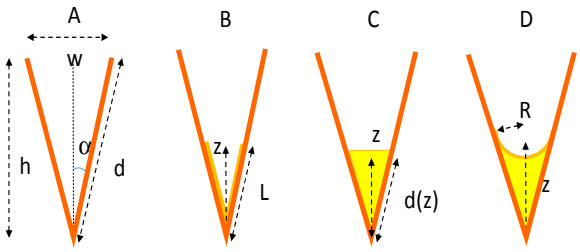

Fig. 11. A: V-groove; B: V-groove with a uniform coating in the dihedral; C: V-groove with trapezoidal coating of the dihedral; D: V-groove with a rounded coating of the dihedral.

The condition (7) for the SCF of reagent is simply the Concus-Finn condition [7]

$$\theta_{R,W} < \frac{\pi}{2} - \alpha\,, \qquad (9)$$

or equivalently

$$\sin\alpha < \cos\theta_{R,W} \qquad (10)$$

Using the trigonometric relations $d = h/\cos\alpha$, $w = 2h\tan\alpha$ and $L = z/\cos\alpha$ – where α is the ½ dihedral angle – we find that in the case (B), the SCF condition for whole blood is

$$\sin\alpha < \cos\theta_{B,W} - \frac{z}{h}\left(\cos\theta_{B,W} - \cos\theta_{B,R}\right) \qquad (11)$$

Using the same arguments, SCF is obtained in case (C) if the inequality

$$\sin\alpha < \cos\theta_{B,W} - \frac{z}{h}\left(\cos\theta_{B,W} - \sin\alpha\cos\theta_{B,R}\right), \quad (12)$$

is satisfied. Finally the last case (D) requires more algebraic developments. We find the SCF condition

$$\sin\alpha < \cos\theta_{B,W}$$
$$-\frac{z}{h}\left[\cos\theta_{B,W} - \left(\frac{\pi}{2} - \left(\alpha + \theta_{B,R}\right)\right)\frac{\sin\alpha}{\cos\left(\alpha + \theta_{B,R}\right)}\cos\theta_{B,R}\right] \quad (13)$$

SCF conditions (11), (12) and (13) are plotted in Fig. 12, assuming that the contact angle between blood and wall and blood and coating are equal, i.e. $\theta_{B,W} = \theta_{B,R}$.

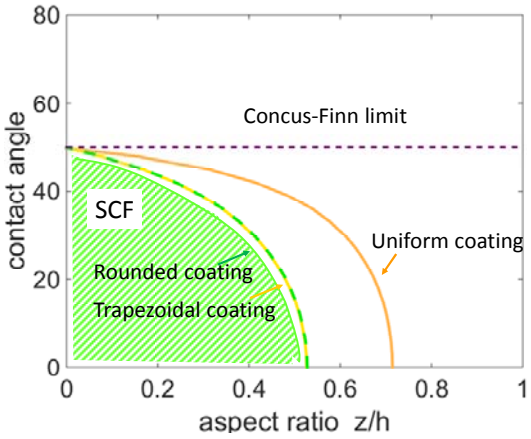

Fig. 12. SCF domains as functions of the coating geometry and contact angle: SCF occurs on the left of the curves; no SCF occurs above a *z*/*h* threshold (case of ½ wedge angle α=40° and $\theta_{B,R}$=60°).

Although the software Surface Evolver does not account for fluid dynamics, it has been shown to produce an accurate determination of the SCF conditions due to the importance of the capillary forces in this type of problems [13, 19, 29, 32]: in particular in [32], it is shown that inertia of the flow can be neglected in front of viscous forces because the Reynolds number is small

$$\mathrm{Re} = \frac{\rho V R}{\mu} < 1, \quad (14)$$

where ρ is the liquid density. Inertia can also be neglected before capillary forces because the Weber number is small

$$We = \frac{\rho V^2 R}{\gamma} < 10^{-4} \quad (15)$$

Finally viscous forces can be neglected before surface tension forces because the Capillary number is small.

$$Ca = \frac{\mu V}{\gamma} < 10^{-3} \quad (16)$$

Hence the flow is governed by surface tension and capillary forces, and Evolver results are a good approximation of the flow. We then use the software Evolver to predict the SCF in channels which corners have been coated by the dried reagent, as shown in Fig. 13 in the case of a V-groove. The Evolve results are found to be in close agreement with the theory.

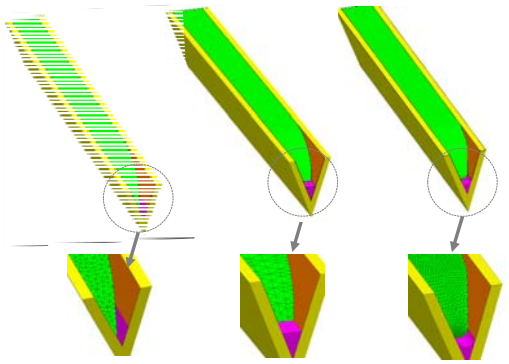

Fig. 13. Evolver calculation of the SCF in V-grooves, depending on the shape of the coating (uniform, triangular or rounded coating/deposit in the wedge (colors: magenta for reagent, brown for naked walls).

5. Discussion and Conclusion

Designing a portable device for blood analysis requires the fulfillement of conditions related to the capillary flow of reagents and whole blood.

In this work, we have analyzed first the non-Newtonian shear rate threshold of whole blood below which whole blood becomes highly viscous. For capillary flows, this threshold corresponds to a channel length limit. It is recommended that the length of the channels be smaller than this threshold length.The spreading of whole blood on different coatings has been experimentally investigated. The spreading dynamic angle is checked to follow the HVT law. A static contact angle has been determined for many blood/reagent couples.

Finally, the conditions for spontaneous capillary flow in V-grooves partially coated with dried reagents is theoretically determined and numerically verified. It is shown that SCF depends on the morphology of the coating and on the blood-reagent contact angle.

Acknowledgements

The authors thank Patricia Laurent (CEA-Leti) for her help for the experiments, and Joanna Spiaczka and Claire Danjean from Avalun (www.avalun.com) for the formulation of the reagents.

References

[1]. P. Yager, T. Edwards, E. Fu, K. Helton, K. Nelson, M. R. Tam, B. H. Weigl, Microfluidic diagnostic technologies for global public health, *Nature*, Vol. 442, No. 7101, 2006, pp. 412-418.

[2]. L. Gervais, N. de Rooij, E. Delamarche, Microfluidic chips for point-of-care immunodiagnostics, *Adv. Mater*., Vol. 23, No. 24, 2011, pp. H151-H176.

[3]. L. Gervais, E. Delamarche, Toward one-step point-of-care immunodiagnostics using capillary-driven microfluidics and PDMS substrates, *Lab Chip*, Vol. 9, No. 23, 2009, pp. 3330-3337.

[4]. J. J. Pirozzolo, D. C. LeMay, Blood-Borne Infections, *Clinics*, Vol. 26, No. 3, 2007, pp. 425-431.

[5]. J. M. Moulds, S. Nowicki, J. J. Moulds, B. J. Nowicki, Human blood groups: incidental receptors for viruses and bacteria, *Transfusion*, Vol. 36, No. 4, 1996, pp. 362-374.

[6]. E. Racila, D. Euhus, A. J. Weiss, C. Rao, J. McConnell, L. W. Terstappen, J. W. Uhr, Detection and characterization of carcinoma cells in the blood, in *Proceedings of the National Academy of Sciences of the United States of America*, Vol. 95, No. 8, 1998, pp. 4589-4594.

[7]. J. Berthier, K. A. Brakke, E. P. Furlani, I. H. Karampelas, V. Poher, D. Gosselin, M. Cubizolles, P. Pouteau, Whole blood spontaneous capillary flow in narrow V-groove microchannels, *Sensors and Actuators B: Chemical*, Vol. 206, 2015, pp. 258-267.

[8]. E. W. Errill, Rheology of blood, *Physiol. Rev*., Vol. 49, No. 4, 1969, pp. 863-888.

[9]. R. Lucas, Ueber das Zeitgesetz des Kapillaren Aufstiegs von Flussigkeiten, *Kolloid-Zeitschrift*, Vol. 23, 1918, pp. 15-22.

[10]. E. W. Washburn, The dynamics of capillary flow, *Physiol. Rev*., Vol. 17, No. 3, 1921, pp. 273-283.

[11]. D. A. Fedosov, Wenxiao Pan, B. Caswell, G. Gomppera, G. E. Karniadakis, Predicting human blood viscosity in silico, *PNAS*, Vol. 108, No. 29, 2011, pp. 11772-11777.

[12]. K. J. Ryan, C. G. George, Sherris medical microbiology: An introduction to infectious diseases (4th ed.), *McGraw Hill*, New York, 2004, pp. 237-242.

[13]. K. A. Brakke, The Surface Evolver, *Experimental Mathematics*, Vol. 1, No. 2, 1992, pp. 141-165.

[14]. W. H. Herschel, R. Bulkley, Konsistenz-Messungen von Gummi-Benzollösungen, *Kolloid-Zeitschrift*, Vol. 39, Issue 4, 1926, pp. 291-300.

[15]. M. P. McEwen, K. J. Reynolds, Light transmission patterns in occluded tissue: Does rouleaux formation play a role?, in *Proceedings of the World Congress on Engineering (WCE'12)*, London, U.K., Vol. 1, 4 – 6 July 2012.

[16]. D. Gosselin, M. Huet, D. Rabaud, M. Cubizolles, J. Berthier, Capillary flow of whole blood: criteria determination of the Newtonian to the non-Newtonian transition, *AIMS Biophysics*, Vol. 2, 2016.

[17]. A. Ahlford, B. Kjeldsen, J. Reimers, A. Lundmark, M. Romani, A. Wolff, A.-C. Syvanen, M. Brivio, Dried reagents for multiplex genotyping by tag-array minisequencing to be used in microfluidic devices, *Analyst*, Vol. 135, No. 9, 2010, pp. 2377-2385.

[18]. J. E. Silva, R. Geryak, D. A. Loney, P. A. Kottke, R. R. Naik, V. V. Tsukruk, A. G. Fedorov, Stick–slip water penetration into capillaries coated with swelling hydrogel, *Soft Matter*, Vol. 11, 2015, pp. 5933-5939.

[19]. J. Berthier, K. Brakke, E. Berthier, A general condition for spontaneous capillary flow in uniform cross-section microchannels, *Microfluid. Nanofluid. Journal*, Vol. 16, Issue 4, 2014, pp. 779-785.

[20]. P. P. Bhat, S. Appathurai, M. T. Harris, M. Pasquali, G. H. McKinley, O. A. Basaran, Formation of beads-on-a-string structures during break-up of viscoelastic filaments, *Nature Physics*, Vol. 6, 2010, pp. 625-631.

[21]. R. L. Hoffman, A study of the advancing interface, Part I: Interface shape in liquid-gas systems, *J. Colloid Interf. Sci*., Vol. 50, No. 2, 1975, pp. 228-241.

[22]. L. H. Tanner, The spreading of silicone oil drop on horizontal surfaces, *J. Phys. D: Appl. Phys*, Vol. 12, 1979, pp. 1473-1484.

[23]. J. Berthier, D. Gosselin, G. Delapierre, Spontaneous Capillary Flow: Should a dynamic contact angle be taken into account?, *Sensors & Transducers*, Vol. 191, No. 8, August 2014, pp. 40-45.

[24]. J. Sung, Y. B. Kim, M. H. Lee, Transient phenomena of dynamic contact angle in microcapillary flow, in *Proceedings of the 15th International Symposium on Flow Visualization*, Minsk, Belarus, 25-28 June 2012.

[25]. V. Siegmund, O. Adjei, P. Racz, C. Berberich, E. Klutse, F. van Vloten, T. Kruppa, B. Fleischer, G. Bretzel, Dry-reagent-based PCR as a novel tool for laboratory confirmation of clinically diagnosed Mycobacterium ulcerans-associated disease in areas in the tropics where M. ulcerans is endemic, *J. Clin. Microbiol*., Vol. 43, No. 1, 2005, pp. 271-276.

[26]. Y. Wang, C. E. Simsa, N. L. Allbritton, Dissolution-guided wetting for microarray and microfluidic devices, *Lab Chip*., Vol. 12, No. 17, 2012, pp. 3036-3039.

[27]. Y. Fuchiwaki, M. Tanaka, H. Takaoka, K. Goya, A capillary flow immunoassay microchip utilizing inkjet printing-based antibody immobilization onto island surfaces – toward sensitive and reproducible determination of carboxyterminal propeptide of type I procollagen, *J. Micromech. Microeng*., Vol. 26, No. 4, 2016.

[28]. P. Concus, R. Finn, On the behavior of a capillary surface in a wedge, *PNAS*, Vol. 63, No. 2, 1969, pp. 292-299.

[29]. J. Berthier, K. A. Brakke, The physics of microdrops, *Scrivener-Wiley Publishing*, Beverly, MA, 2012.

[30]. M. Kitron-Belinkov, A. Marmur, T. Trabold, G. V. Dadheech, Groovy-drops: effect of groove curvature on spontaneous capillary flow, *Langmuir*, Vol. 23, No. 16, 2007, pp. 8406-8410.

[31]. P. Casavant, E. Berthier, A. B. Theberge, J. Berthier, S. I. Montanez-Sauri, L. L. Bischel, K. Brakke, C. J. Hedman, W. Bushman, N. P. Keller, D. J. Beebe, Suspended microfluidics, *PNAS*, Vol. 110, No. 25, 2013, pp. 10111-10116.

[32]. J. Berthier, K. Bakke, D. Gosselin, F. Navarro, N. Belgacem, D. Chaussy, Spontaneous capillary flow in curved, open microchannels, *Microfluid. Nanofluid*., Vol. 20, Issue 7, 2016, p. 100.